PROCEEDINGS OF SPIE

Linear and nonlinear optical properties of highly transmissive one-dimensional metal-organic photonic bandgap structures

Fuentes-Hernandez, Canek, Padilha, Lazaro, Owens, Daniel, Tseng, Shuo-Yen, Webster, Scott, et al.

SPIE.

Linear and nonlinear optical properties of highly transmissive one-dimensional metal-organic photonic bandgap structures

Canek Fuentes-Hernandez,*[a] Lazaro A. Padilha,[b] Daniel Owens,[a] Shuo-Yen Tseng,[a] Scott Webster,[b] Jian-Yang Cho,[c] David J. Hagan,[b] Eric W. Van Stryland,[b] Seth R. Marder,[c] Bernard Kippelen[a]

[a] Center for Organic Photonics and Electronics, School of Electrical and Computer Engineering, Georgia Institute of Technology, Atlanta, GA 30332;
[b] CREOL & FPCE, College of Optics and Photonics, University of Central Florida, Orlando, FL, 32826;
[c] Center for Organic Photonics and Electronics, School of Chemistry and Biochemistry, Georgia Institute of Technology, Atlanta, GA 30332;

ABSTRACT

We present the design, fabrication and characterization of the optical properties of one-dimensional metal-organic photonic bandgaps (MO-PBGs) composed of a tetraphenyldiaminobiphenyl-based polymer and ultrathin electrically continuous Cu layers. The fabricated MO-PBGs achieve a peak transmission of around 44% at 620 nm combined with very large spectral, around 120 nm FWHM, and angular, more than 120° field-of-view, bandwidths. Using 140 fs pulses at various wavelengths we have found up to 10 × enhancements in the nonlinear optical (NLO) properties of the MO-PBGs when compared with the NLO response of ultrathin electrically continuous Cu layers.

Keywords: noble metals, metal-organic photonic band gaps, nonlinear optical properties

1. INTRODUCTION

The extremely large nonlinear optical (NLO) response of metals such as Au,[1,2] Ag,[3] and Cu[4] makes them very attractive for broadband optical switching devices in the visible (VIS) and near-infrared (NIR) spectral ranges. However, electrically continuous metallic films only a few nanometers thick, around the metal's skin depth, produce a strong attenuation of the optical fields either by absorption or reflection. At visible frequencies, the optical properties of noble metals are dominated by contributions due to interband transitions, from the d-band to the conduction band, or by intraconduction band transitions ("free" electron absorption). Across this range, the attenuation coefficient ($\mathrm{Im}\{n\} = \kappa$) dominates over the refractive index ($\mathrm{Re}\{n\} = n_0$) and produces a negative permittivity, leading to a very large permittivity contrast with respect to any dielectric material. This makes it possible to engineer compact structures, such as metal-dielectric photonic band gaps (MD-PBGs),[5] with transparency windows in the VIS and NIR that achieve larger photonic band gaps (PBGs) than is possible with combinations of dielectrics.[6,7] Opening such transparency windows also leads to an increased optical-field density within the metallic layers and yields the possibility of accessing and amplifying their NLO response.[8] While this approach has been demonstrated using MD-PBGs that contain Cu,[9] Ag[10,11] and Au,[12] the selection of dielectrics and the structural design have led to peak transmissions below 20 % and to moderate enhancements of the metal's NLO response. Additionally, knowledge of the NLO response of bulk metals and their spectral dispersions remain elusive because the limited transmission through continuous metallic layers has made it difficult to directly measure the NLO response with standard techniques such as Z-scan or degenerate four-wave mixing, and because the NLO response of metals with nanometer-size dimensions is strongly dependent on morphology, dielectric environment,[13] and the temporal width of the optical excitation.[1] However, thermomodulation experiments provide evidence that the strongest contribution to the NLO response of metals should arise from the temperature dynamics of electrons upon optical excitation, and the different ways in which these thermal changes modify the metal's permittivity.[14] When ultra-short pulses of large fluence are absorbed by the metallic layers, the electron temperatures can increase by several thousands of degrees and the lattice temperatures by several tens of degrees.[15] Hence, the use of organic materials such as polymers[12] is desirable because its thermo-elastic properties should be better matched than inorganic dielectrics to deal with the large temperature gradients that can be created in these structures and because,

*canek@ece.gatech.edu phone 1 404 385-6288; fax 1 404 385-5168

given the chemical flexibility of organic materials, it could open up new paths for the design of all-optical and electro-optic devices.

In this paper, we investigate the design and fabrication of MO-PBGs that use a tetraphenyldiaminobiphenyl-based polymer (PTPD) and Cu to achieve a peak transmission of around 44% at 620nm, combined with large spectral and angular bandwidths. Using closed and open aperture Z-scan experiments with 140 fs pulses at 570 nm and 700 nm we investigate the complex NLO response of such MO-PBG and two substructures and compare it with that of a continuous Cu film. We demonstrate up to an order of magnitude enhancement of the Cu NLO response by use of the MOPBG structure.

2. MATERIAL CHARATERIZATION

2.1 Linear optical properties of PTPD and Cu
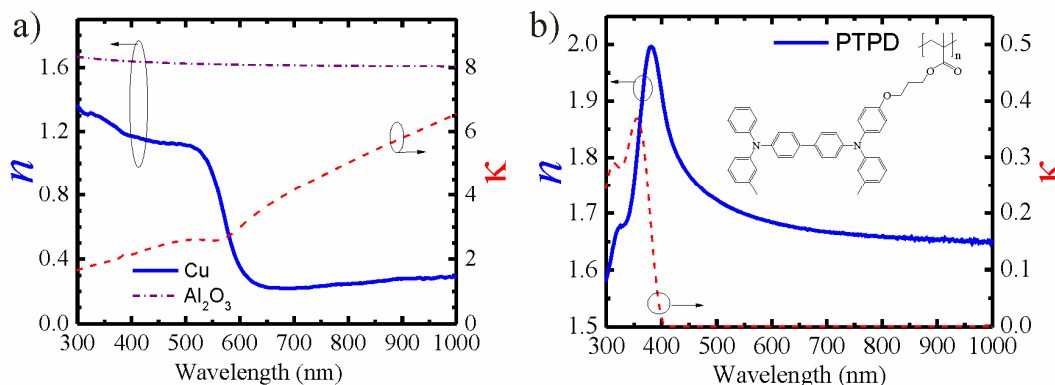
Fig. 1. Linear index of refraction of: a) Cu and Al_2O_3 (κ negligible in measured range) and b) PTPD measured by spectral ellipsometry. Inset of b) shows the chemical structure of PTPD.

The "bulk" refractive index of Cu, Al_2O_3 and PTPD was measured using a Woollam M-2000 spectroscopic ellipsometer operating in reflection mode. Copper and Al_2O_3 were deposited under vacuum ($<10^{-6}$ Torr) using a Kurt J. Lesker Axxis electron beam (e-beam) deposition system equipped with a rotating and actively-cooled substrate holder that kept the substrates at room temperature. For Cu and Al_2O_3, ellipsometric measurements were carried out immediately after e-beam deposition. A 100 nm thick Al_2O_3 layer deposited at 0.2 nm/s and a 50 nm thick Cu layer deposited at 0.1 nm/s onto pre-cleaned Si substrates were used for the refractive index characterization. Figure 1a) shows the measured refractive index of Cu, which is in good agreement with published values for bulk Cu. Also shown in Fig. 1a) is the refractive index of Al_2O_3, which is important to characterize because it can vary significantly depending on deposition and environmental conditions.[16] The attenuation coefficient of Al_2O_3 is negligible throughout the VIS range. Polymeric layers were spin-casted in air using a Laurell Technologies Co. WS-400B06NPP/LITE spin-coater. To measure PTPD's refractive index, an 80 nm thick layer was spin-casted onto a Si-wafer at 2000 rpm from a 20 mg/ml solution in Toluene. As shown in Fig. 1b), PTPD shows negligible optical losses through most of the VIS spectral range. However, with an absorption peak at 355 nm, PTPD has a significantly more dispersive refractive index than Al_2O_3.

Figure 2a) shows that the transfer matrix (TM) method[17] can effectively be used to simulate the linear transmittance of a multilayer structure provided the index of refraction of the different layers is known. In such simulations the thickness can be taken as the sole fitting parameter. Estimations of the layer thicknesses using this method are in excellent agreement with spectroscopic ellipsometric (SE) measurements and with direct measurements using a Dektak 6M stylus profilometer. As shown in Figure 2, electrically continuous Cu layers around 10 nm thick can be successfully deposited by e-beam on Al_2O_3 and PTPD. Its electrical continuity was confirmed over the 1×1 inch area of the samples through measurements of a finite resistance ($< 5\ \Omega$) with a standard multimeter. The good agreement obtained between the experimental and simulated transmission using Cu's "bulk" refractive index values, and the surface characterization using scanning electron microscopy (SEM) and atomic force microscopy (AFM), as shown in Figure 2b), provided further evidence of the continuity of the layers. Small differences in transmittance between experimental and simulated

values, most likely can be accounted for by surface roughness effects and the unavoidable oxidation of the Cu surface upon exposure to air. Using AFM, a root-mean squared (RMS) surface roughness of 1.1 nm was estimated for the Cu on Al_2O_3 layer. For Cu on PTPD an RMS surface roughness of ~ 0.6 nm was estimated, clearly showing that PTPD acts as a planarization layer. Given the environmental conditions and the time elapsed between the fabrication of the Cu layers and the optical measurements, the thickness of the oxide layer at the surface is estimated to be around 1 nm.[18] Figure 2b) also shows a slight difference in the morphology of Cu deposited on PTPD, where a uniform distribution of small grains contrasts with a distribution of larger domains of uniform height in the Cu layers deposited on Al_2O_3. Despite these subtle morphological differences, the linear optical properties within the VIS spectral range of these thin, continuous Cu layers are not significantly different from those of the bulk. When thinner Cu layers are deposited, the linear optical properties can no longer be described by bulk refractive index values because plasmonic effects start to dominate the optical spectra in the form of an enhanced broadband absorption and an increased refractive index for wavelengths above the onset of interband transitions, which in Cu lies around 2.15 eV (577 nm).

The ability to deposit these ultrathin Cu layers, thinner than the skin depth (12 nm in the VIS for Cu), on top of these different materials allows the implementation of PBG designs that potentially could have higher transmittance and broader spectral bandwidths than those achieved with thicker metal layers. Moreover, it enables the fabrication of Cu samples that are transparent enough for NLO characterization with standard transmission techniques, such as Z-scan.[19] As shown in Fig 2a), a 10 nm thick continuous Cu layer shows more than 40 % transmittance in the VIS range. It has the typical spectral signature of a continuous metal, with a transparency window around the onset of interband transitions that is limited on the blue edge by absorption due to interband transitions from the *d*-band to the conduction band, and on the red edge by the large reflectivity arising from the low refractive index in the "free" electron region and, to a smaller degree, by the broadband absorption produced by intraband transitions of "free" electrons within the conduction band.
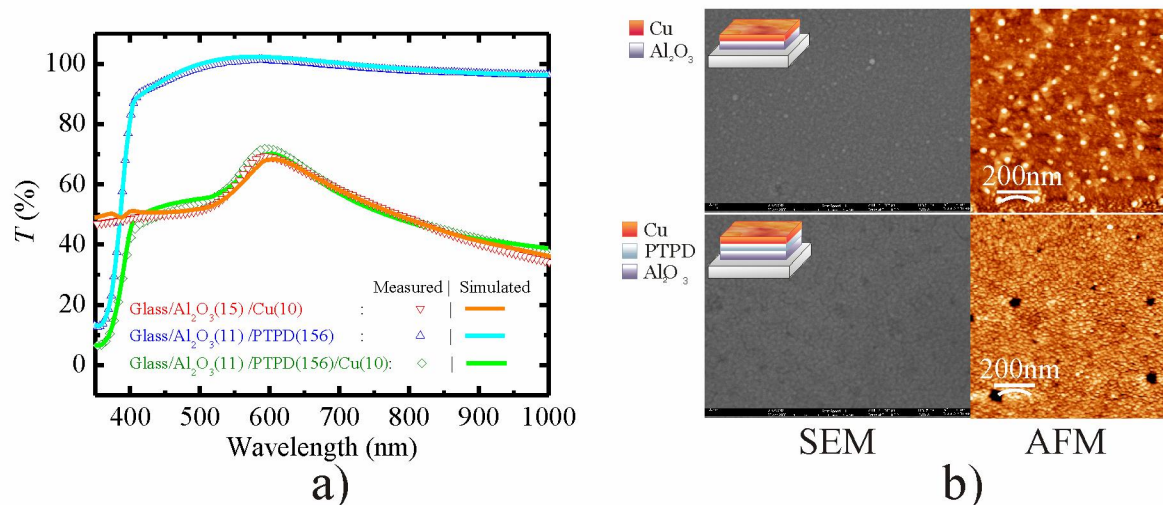
Fig. 2. a) Experimental (symbols) and simulated (lines) transmittance of PTPD spin-casted on Al_2O_3/Glass, and of 10 nm Cu layers deposited on Al_2O_3 /Glass and PTPD/ Al_2O_3/Glass substrates, and b) the corresponding SEM and AFM images showing a total span of 1 μm in the horizontal direction . The thicknesses shown in a) are in nm, and correspond to the best fits to the measured optical transmittance using the TM method.

2.2 MOPBG design

Figure 3 shows the structure and simulated optical properties of the targeted MO-PBG. As shown in Fig. 3b), the linear optical properties of such structures are designed to be similar to those of a "bulk" Cu layer: a large absorption closer to the blue edge of the transmittance window and an increasingly large reflectivity approaching the red edge. Despite having an accumulated Cu mass thickness of 48 nm, the MO-PBG yields a peak transmission of 50%, equivalent to that of a continuous 17 nm thick Cu layer and ~ 5.5 times larger than that expected from a continuous 48 nm Cu layer.
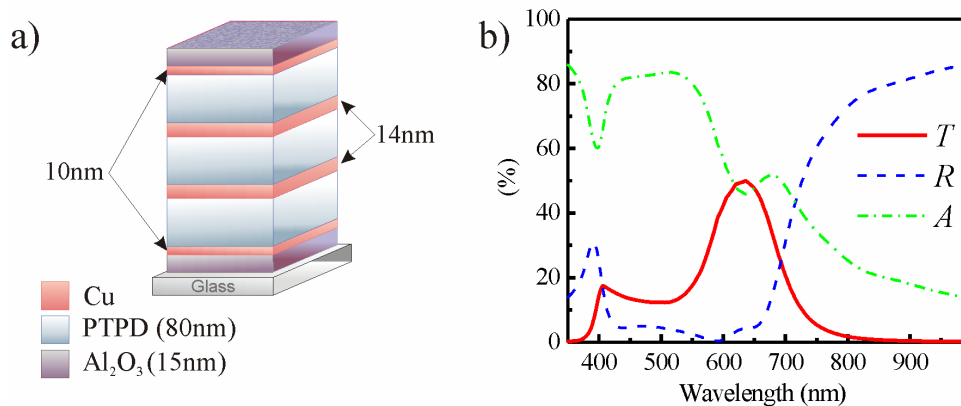
Fig. 3. a) Structure of Cu:PTPD based MOPBG; b) Simulated transmittance (T), reflectance(R) and absorbance(A) of targeted MOPBG using the TTM;

In the linear regime, MO-PBGs can be thought of as stacked metal/organic/metal Fabry-Perot resonators with very low finesse. Because of the strong metal absorption, the condition for resonant transmission becomes $m\lambda_{peak} = 2\,n_p\,t_p - \phi_1 - \phi_2$, where n_p and t_p are the refractive index and thickness of the organic layer, while ϕ_1 and ϕ_2 are the phase shifts accumulated by the backward and forward propagating fields inside each cavity upon multiple reflections throughout the structure. Therefore, the dielectric thickness required for the first order resonance, $m = 1$, no longer is given by the common condition $\lambda_{peak}/2n_o$. For the range of metal thicknesses used in our structure, this condition is in fact closer to $\lambda_{peak}/4n_o$. The central resonance of the structure was tuned at around 630 nm, slightly red shifted from the onset of interband transitions but close enough to take advantage of the natural transparency window around it while eliminating the spectrally sharp resonances that are typically observed within the broad transmission passband ($\Delta\lambda_{FWHM} \sim 120$ nm) of MD-PBGs.[20] The increased thickness of the internal Cu layers was found to reduce the reflectivity of the structure within the passband. The presence of the Al_2O_3 layers was primarily motivated by the fabrication process because it provided a reproducible surface energy match that allowed the reliable deposition of the first continuous Cu layer, and because they acted as efficient anti-oxidation barriers for the MO-PBG structure (the fabricated MO-PBGs have shown environmental stability for over 10 months). Additionally, their presence reduced the reflectivity of the MO-PBG, which is the single most important parameter in optimizing its linear transmission.

Through DFWM measurements on Cu-nanoparticle doped glasses in the ns regime a value of $\chi^{(3)} \sim 10^{-6}$ *esu* for bulk Cu was estimated.[21] Using this value and Cu-based MD-PBG structures with similar linear optical properties to the one reported in this paper, theoretical predictions in the literature have been made of very strong nonlinear phase shift enhancements with respect to bulk Cu,[8] and even the possibility of broadband nonlinear transmittance devices in the ps temporal regime.[22] However, the only Cu-SiO$_2$ based PBG fabricated, investigated in the ps regime, showed a limited peak transmission of ~ 20 % and about an order of magnitude enhancement in the nonlinear absorption.[9] The lack of a detailed NLO characterization of bulk Cu along the VIS range, and the strong pulse-width dependence of the NLO response of noble metals,[1] makes it difficult at this point to develop a clear strategy for the optimization of the MO-PBG NLO response. Thermomodulation experiments, in fact, may provide the best evidence of the strong effects that the absorption of ultrafast optical pulses bring to the thermal dynamics of electrons and their effects on the dielectric permittivity of continuous metal layers,[15,23] as well as on the critical role that the pulse width and the thermal properties of the substrate layers play in controlling the magnitude of such thermal modulations.[24] Recently, the first attempts to relate these effects to the signals obtained through Z-scan experiments were reported for the analysis of the nonlinear absorption on thin gold films using a wide range of pulse widths.[1] Clear correlation of the experimental traces with the variations expected through a thermomodulation analysis indicated that the nonlinear absorption coefficient β_{eff} observed in Au is dominated by thermally induced changes to the linear absorption of the metal, Im$\{\chi^{(1)}\}$. This is in good agreement with experimental observations[8,12] that correlate enhancements of β_{eff} in MD-PBG structures with the increase in the linear absorption with respect to the bulk. Hence, enhancements are related to the degree in which the optical field density is increased within the metallic layers by virtue of the PBG structure in the linear regime. Expressed as an

intensity sensitive factor,[8] it can be defined as the ratio between the spatial average of the square of the optical field within the metallic layers in the MDPBG and that in a "bulk" sample:

$$F(\lambda) = \left\langle |E_m|^2 \right\rangle_{MOPBG} \Big/ \left\langle |E_m|^2 \right\rangle_{bulk} . \tag{1}$$

Solving numerically Maxwell's [8,9,12] equations for H and E for our MO-PBG structure, and compared to a 48 nm thick Cu layer sandwiched between 15 nm Al_2O_3 layers, we estimated $F(\lambda) \sim 2$ and 9.9 at 570 and 700 nm respectively. Hence enhancements of β_{eff} in this range could be expected. It's worth pointing out that β_{eff} is commonly associated with two-photon absorption. However, in metals no such physical meaning can be ascribed. Rather, β_{eff} should be understood as the parameter associated with the first order approximation to the experimentally measured irradiance dependence of the absorption in the metal.

2.3 MOPBG fabrication

1x: G| D(15)/M(9.5)/O(77)/M(9.5)/D(15),
2x: G| D(15)/M(10)/O(77)/M(15.5)/O(102)/M(10)/D(15),
3x: G| D(15)/M(10)/O(77)/M(14)/O(77)/M(14)O(100)/M(10)//D(15).
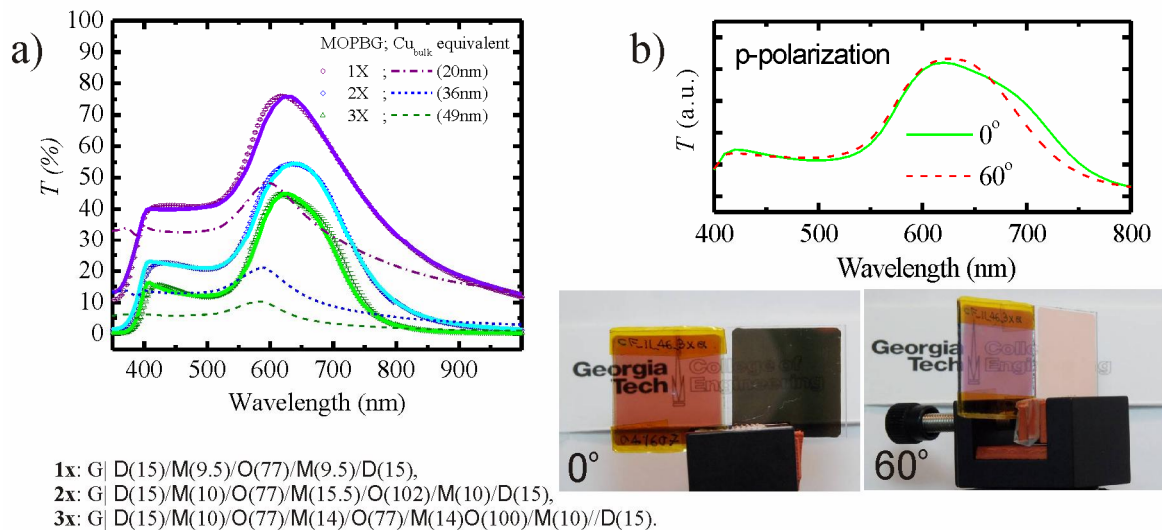
Fig. 4. a) Experimental (symbols) and simulated (lines) linear transmittance of samples **1x**, **2x** and **3x** and the simulated transmittance of "equivalent" thickness Cu layers. On the bottom, the thicknesses (nm) used for the simulations; b) Measured transmittance, p-polarized light, at normal incidence and at incidence angle of 60° on sample **3x**. At the bottom, pictures show sample **3x** and a 50 nm thick Cu layer at the same angles but under room lights.

The targeted MO-PBG structure was fabricated by successive depositions using the techniques and experimental methods described in section 2.1. The simultaneous fabrication of multiple samples allowed step-by-step monitoring of the fabrication process as well as producing several substructures of the MO-PBG which could be used for the NLO characterization. The targeted substructures, with the dimensions given in nm, had the following structure:

Cu: G|D(15)/M(10)/D(15)| Air,

1x: G|D(15)/M(10)/O(80)/M(10)/D(15)| Air,

2x: G|D(15)/M(10)/O(80)/M(14)/O(80)/M(10)/D(15)| Air,

where G corresponds to glass, D to Al_2O_3 , M to Cu and O to PTPD. The name given to the substructures makes reference to the number of resonant cavities (metal/polymer/metal) contained in its geometry. Following this convention, sample **3x** refers to the MO-PBG as described in Fig. 3a). Sample **Cu** was deposited separately from the rest and without breaking vacuum between depositions. On samples **1x**, **2x** and **3x**, e-beam depositions of the inorganic layers were carried out simultaneously under vacuum, but samples had to be exposed to air to allow spin coating of the polymer layers. Since measurement of the linear transmittance of most sequentially deposited Cu and PTPD layers was possible, the thickness of each layer was estimated using the TM method. To minimize sample exposure to air, such transmittance measurements were carried out on Cu and PTPD layers fabricated simultaneously with the targeted samples but on different glass substrates. The linear transmittance on samples **1x**, **2x** and **3x,** shown in Figure 4a), was measured only

after the entire structures were completed. Thickness estimations on independent samples were used as starting guesses to fit the transmission on the targeted samples. In all cases, estimated thickness values didn't vary more that 10 % before agreement with the experimental data was obtained, validating the good spatial homogeneity of the e-beam system, and the relatively good reproducibility of the polymer deposition. Figure 4a) shows the simulated transmittance along with the corresponding thicknesses used for the simulations. With the exception of the last polymer layer, agreement with respect to the targeted values was obtained. Hence, the smaller peak transmission and broader spectral bandwidth obtained in sample **3x** can successfully be explained solely by thickness differences with respect to the targeted values. To demonstrate the small angular sensitivity of sample **3x**, the transmittance under p-polarized light was measured at normal incidence and at an incidence angle of around 60°, as shown in Fig. 4b). The single structural resonance and the small reflectivity within the transmission window produce a very wide field-of-view (> 60 degrees). At the bottom of Fig. 4b) are pictures of the fabricated MO-PBG, showing the good homogeneity of the 1x1 inch sample, alongside a 50 nm Cu layer.

3. NONLINEAR OPTICAL PROPERTIES

The NLO properties of all samples were measured using closed and open aperture Z-scan experiments[19] implemented with an optical parametric amplifier producing 140 fs pulses (FWHM) at a repetition rate of 1 kHz with energies in the range from 2 - 45 nJ at 570 nm and 700 nm. For the analysis of sample **Cu**, a 10 cm focal length lens was used to focus down the beam to a focal spot size (HW/e^2) of 18.5 μm and 18.6 μm at 570 nm and 700 nm respectively. For the rest of the samples, a 15 cm focal length lens was used, producing a focal spot size of 13.8 μm and 15.6 μm at 570 nm and 700 nm respectively. Values for the irradiance at the sample were calculated taking into consideration Fresnel losses, simulated by the TM method using the thickness values described in Fig. 4a). The index of refraction and absorption coefficients were defined as $n(I) = n_0 + n_{2,eff} I_0$ and $\alpha(I) = \alpha_0 + \beta_{eff} I$. By fitting[19] the experimental Z-scan traces we calculated $\Delta\Phi_0 = k \, n_{2,eff} L_{eff} I$ and $q_0 = \beta_{eff} L_{eff} I$, where $k = 2\pi/\lambda$ is the wave vector, $L_{eff} = [1 - \exp(-\alpha_0 d)]/\alpha_0$ is the effective length, d is the sample length, and I is the irradiance. As mentioned previously, the nonlinear refraction and absorption have been defined as a first order approximations to the measured irradiance dependence.

3.1 Nonlinear optical properties

Figure 5 shows open and closed aperture Z-scan measurements at 570 nm and 700 nm for samples **Cu** and **3x**. Two distinctive features are evident: 1) the sign difference on the nonlinear refraction in **Cu**, negative ($n_{2,eff} < 0$) at 570 nm and positive ($n_{2,eff} > 0$) at 700nm, carries over into the NLO response of sample **3x**; and 2) the NLO response of sample **3x** is clearly larger compared to that of sample **Cu**. In sample **Cu**, the effective nonlinear refraction and absorption coefficients were estimated to be $n_{2,eff} = (-2.4\pm0.7)\times10^{-11}$ cm^2/W and $\beta_{eff} = (6\pm2)\times10^{-6}$ cm/W at 570 nm, while at 700 nm $n_{2,eff} = (2.9\pm0.5)\times10^{-11}$ cm^2/W and $\beta_{eff} = (1.8\pm0.4)\times10^{-6}$ cm/W. These values were confirmed independently at 570 nm using a 20 nm Cu layer sandwiched between 15 nm Al$_2$O$_3$ layers. At 700 nm reliable data could not to be obtained; however, the magnitude of β_{eff} is on the same order of magnitude as values recently reported for Au thin films using pulses widths on the fs time scale and at a wavelength with a similar offset with respect to the interband transition in Au.[1] In sample **Cu**, the presence of the Al$_2$O$_3$ layers increase $<|E_z|^2>$ by around 15% at both wavelengths, a correction that is within the experimental uncertainty. Differences in sign and magnitude of the NLO response of Cu at the different wavelengths are most likely related to the different mechanisms leading to the change in the dielectric permittivity of the metal at different wavelengths. At 700 nm, the off-resonance contribution of intraband transitions should lead to smearing of the Fermi distribution due to the creation of a hot electron distribution upon absorption which, at the ps time scale, dissipates its energy to the lattice through electron-phonon interactions. Changes to the dielectric constant are expected to be dominated by changes in the imaginary part of the interband contribution and to a smaller degree affected by changes in the free electron contribution due to thermal changes in the electron-electron scattering rate.[25] At 570 nm, the resonant contribution of interband transitions should produce a population change around the Fermi energy by decreasing the occupation number of states below E_F, therefore reducing absorption for transitions involving final states above the Fermi level.[26] Unlike previous reports, we have been able to measure the nonlinear refractive response of bulk Cu, so we expect that further analysis will reveal the proper way to interpret Z-scan traces with respect to the expected thermal changes on the dielectric permittivity of the metal. It is worth pointing out that at the measured wavelengths and temporal range, the magnitude of nonlinear refractive index changes is comparable to that of nonlinear absorption changes and can not be neglected. Z-scan experiments carried out in 500 nm thick PTPD samples at both wavelengths show no measurable NLO response at the selected wavelengths. Hence, the NLO response observed in sample **3x** is dominated by the Cu layers.
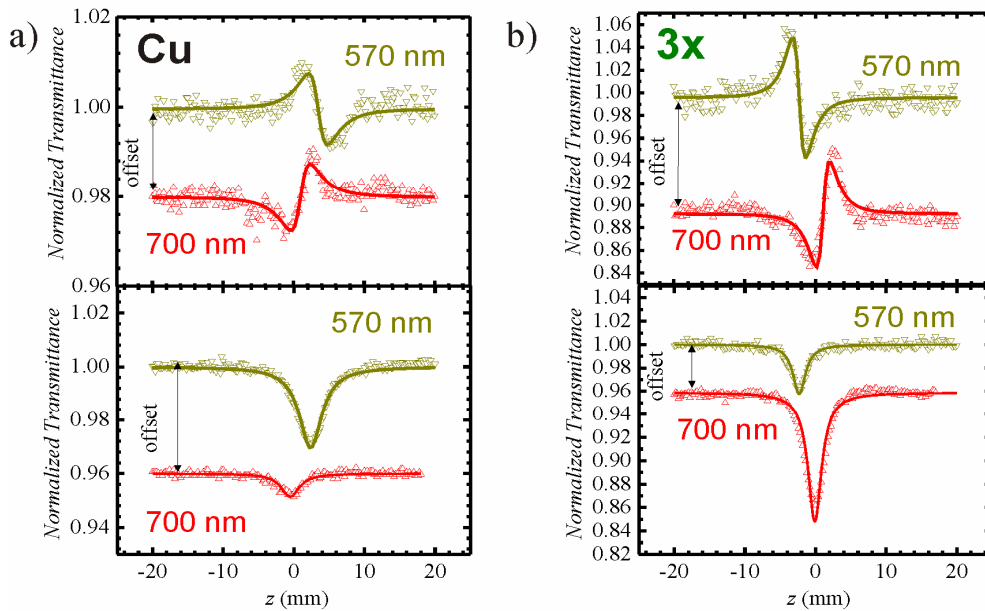
Fig. 5. Experimental (symbols) and fitted (lines) closed (top) and open (bottom) aperture Z-scan traces for: a) sample **Cu** and b) sample **3x** (MO-PBG). For clarity an arbitrary offset has been introduced for the traces at 700 nm. An incident energy of 20 nJ, before Fresnel losses, was used for all traces shown except for the open aperture experiments for sample 3x (bottom right), taken at 10 nJ.

In contrast with bulk Cu, where $n_{2,eff}$ and β_{eff} are clearly defined, in a MO-PBG these parameters lack significant meaning since they can not account for the resonance response of its structure. Hence, a comparison between the NLO response of bulk Cu and samples **1x**, **2x** and **3x**, is better made by comparing directly $\Delta\Phi_0$ and q_0. As seen in Fig. 6a), within the measured range, in all samples, $\Delta\Phi_0$ follows approximately a linear irradiance dependence. A similar trend was observed at 570 nm. The nonlinear phase shift expected from bulk Cu layers, $(\Delta\Phi_0)_{bulk}$, with a total mass thickness equal to that contained in samples **1x**, **2x** and **3x** respectively, was extrapolated using $n_{2,eff}$ measured in sample **Cu** and L_{eff} estimated from SE experiments. The thicknesses used in these extrapolations were 20 nm, 36 nm and 49 nm. The extrapolated values expected for such layers are also plotted as discontinuous lines in Fig. 6a). The enhancement factor for the refractive nonlinear phase shift, defined as the ratio $(\Delta\Phi_0)_{MO-PBG}/(\Delta\Phi_0)_{bulk}$, is shown in Fig. 6b) at the measured wavelengths. A similar procedure was followed to analyze open aperture Z-scan experiments. At the bottom of Fig. 6a), the normalized transmission at the focal position is shown as a function of irradiance. Solid lines were obtained by plotting: $T(z) = \dfrac{1}{\sqrt{\pi}\, q_0} \displaystyle\int_{-\infty}^{\infty} \ln\left[1 + q_0 e^{-t^2}\right] dt$, using the same q_0 values obtained by fitting open aperture Z-scan traces. To estimate $(q_0)_{bulk}$ we used the value of β_{eff} measured in sample **Cu** and L_{eff} from SE measurements. The nonlinear absorption enhancement factor $(q_0)_{MO-PBG}/(q_0)_{bulk}$ is shown in Fig. 6b) at both measured wavelengths. At 700 nm, nonlinear absorption is enhanced by an order of magnitude with respect to the expected value in a 49 nm thick Cu layer while the enhancement of the nonlinear refraction term is only a factor of 2.6 on the **3x** sample. The enhancement on the nonlinear absorption quantitatively correlates closely to the previously defined intensity sensitive factor F, as shown in Fig. 6b) and qualitatively with the nonlinear refraction enhancement term. If we describe nonlinear propagation at this wavelength by assuming that refractive index changes arise from a $\chi^{(3)}$ process, using the nonlinear refraction and absorption coefficients obtained on sample **Cu**, we can estimate: $\chi^{(3)}_{eff}(700\ nm) \sim (-2 + 6.8\ i) \times 10^{-10}\ esu$. Using $\chi^{(3)}_{eff}(700\ nm)$ and numerically solving Maxwell equations[8,9,12] reasonable agreement is obtained with the experimental values, considering that the model considers only continuous wave propagation. However, at 570 nm enhancements do not correlate directly with F and the cw model predicts an increased transmittance with increasing irradiance. Hence, both approximations fail to predict the decrease in the transmittance observed.
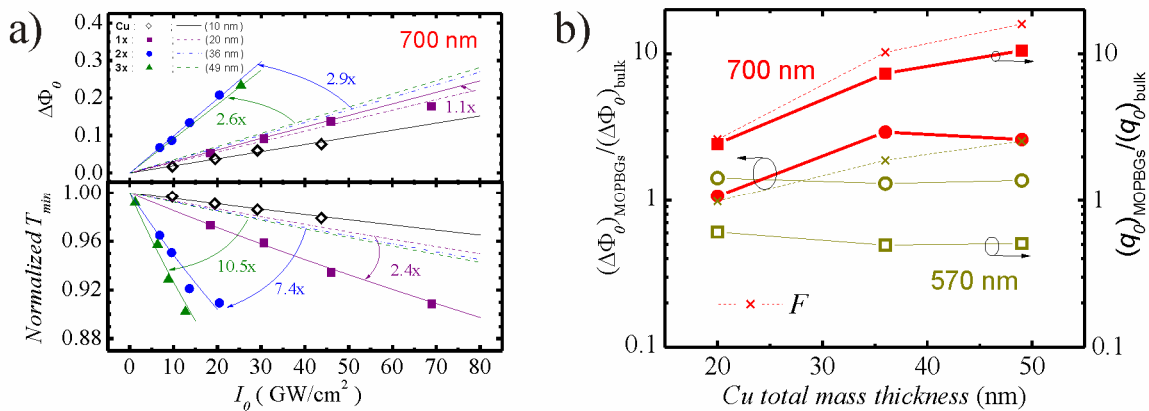
Fig. 6. a) Irradiance dependence at 700 nm of nonlinear phase-shift and normalized transmission at the focal position ($z = 0$) for samples **Cu, 1x**, **2x** and **3x**. Lines are fits to the data and the extrapolated response of Cu layers with and equivalent thickness to the 1x, 2x and 3x samples; b) Summary of enhancement factors as a function of the total Cu mass thickness at 700 nm (red symbols) and at 570 nm (yellow symbols); lines are just a guide to the eye. The intensity sensitive factor F, recalculated using the estimated thickness is also shown (x) for both wavelengths.

4. CONCLUSIONS

We have designed and fabricated an MO-PBG that combines a large linear transmittance, with a peak transmittance of ~ 44 %, with broad spectral and angular bandwidths. The nonlinear optical properties of the MO-PBG were investigated using Z-scan experiments, at 570 nm and 700 nm, and its response compared with bulk Cu layers. At 700 nm, on the red side of the passband, we have found that the nonlinear absorption in the MO-PBG is enhanced by around an order of magnitude with respect to that expected in bulk Cu. This enhancement correlates with the increased linear absorption within the MOPBG structure. However, on the blue edge of the passband, at 570 nm, the nonlinear absorption is reduced when compared with bulk Cu and experimental results can no longer be explained with the simple models proposed in the literature. A decreasing transmittance with increasing input irradiance was observed at both wavelengths. While these changes are relatively small considering the large irradiance required, the fact that the nonlinear response of metals scales with the temporal width of the optical excitation could make these changes quite significant in the ps and ns temporal regimes, and structures like the presented MO-PBG attractive for broadband all-optical switching applications. While we are more interested in enhancing the nonlinear absorption of Cu because of its potential for all-optical switching applications, the magnitude of the nonlinear refractive changes in Cu and in the MO-PBG revealed by our measurements, is comparable to nonlinear absorption changes, so its effects can not be overlooked and potentially could be used to our advantage when designing these structures. Making the connection between the nonlinear optical response in bulk noble metals, commonly discussed in terms of a $\chi^{(3)}$ contribution, and the thermal changes of the dielectric function which are related to $\chi^{(1)}$ changes, is critical if accurate models are to be developed to predict the real potential of these PBG structures.

REFERENCES

[1]   N. Rotenberg, A. D. Bristow, M. Pfeiffer, M. Betz, and H. M. Van Driel, "Nonlinear Absorption in Au Films: Role of Thermal Effects," Phys. Rev. B **75** (15), 155426 (2007).

[2] D. D. Smith, Y. Yoon, R. W. Boyd, J. K. Campbell, L. A. Baker, R. M. Crooks, and M. George, "Z-Scan Measurement of the Nonlinear Absorption of a Thin Gold Film," J. Appl. Phys. **86** (11), 6200 (1999).

[3] G. Yang, D. Y. Guan, W. T. Wang, W. D. Wu, and Z. H. Chen, "The Inherent Optical Nonlinearities of Thin Silver Films," Opt. Mater. **25** (4), 439 (2004).

[4] T. Tokizaki, A. Nakamura, S. Kaneko, K. Uchida, S. Omi, H. Tanji, and Y. Asahara, "Subpicosecond Time Response of Third-Order Optical Nonlinearity of Small Copper Particles in Glass," Appl. Phys. Lett. **65** (8), 941 (1994).

[5] M. M. Sigalas, C. T. Chan, K. M. Ho, and C. M. Soukoulis, "Metallic Photonic Band-Gap Materials," Phys. Rev. B **52** (16), 11744 (1995).

[6] S. H. Fan, P. R. Villeneuve, and J. D. Joannopoulos, "Large Omnidirectional Band Gaps in Metallodielectric Photonic Crystals," Phys. Rev. B **54** (16), 11245 (1996).

[7] J. G. Fleming, S. Y. Lin, I. El-Kady, R. Biswas, and K. M. Ho, "All-Metallic Three-Dimensional Photonic Crystals with a Large Infrared Bandgap," Nature **417** (6884), 52 (2002).

[8] R. S. Bennink, Y. K. Yoon, R. W. Boyd, and J. E. Sipe, "Accessing the Optical Nonlinearity of Metals with Metal-Dielectric Photonic Bandgap Structures," Opt. Lett. **24** (20), 1416 (1999).

[9] N. N. Lepeshkin, A. Schweinsberg, G. Piredda, R. S. Bennink, and R. W. Boyd, "Enhanced Nonlinear Optical Response of One-Dimensional Metal-Dielectric Photonic Crystals," Phys. Rev. Lett. **93** (12), 123902 (2004).

[10] M. C. Larciprete, C. Sibilia, S. Paoloni, M. Bertolotti, F. Sarto, and M. Scalora, "Accessing the Optical Limiting Properties of Metallo-Dielectric Photonic Band Gap Structures," J. Appl. Phys. **93** (9), 5013 (2003).

[11] G. J. Lee, Y. Lee, S. G. Jung, B. Y. Jung, C. K. Hwangbo, S. Kim, and I. Park, "Design, Fabrication, Linear and Nonlinear Optical Properties of Metal-Dielectric Photonic Bandgap Structures," J. Kor. Phys. Soc. **51** (1), 431 (2007).

[12] T. K. Lee, A. D. Bristow, J. Hubner, and H. M. Van Driel, "Linear and Nonlinear Optical Properties of Au-Polymer Metallodielectric Bragg Stacks," J. Opt. Soc. Amer. B **23** (10), 2142 (2006).

[13] V. M. Shalaev, in *Topics in Applied Physics*, edited by Ascheron, C. E. (Springer-Verlag, Berlin Heidelberg, 2002), Vol. 82, p. 450.

[14] R. Rosei and D. W. Lynch, "Thermomodulation Spectra of Al, Au, and Cu," Phys. Rev. B **5** (10), 3883 (1972).

[15] H. E. Elsayed-Ali, T. B. Norris, M. A. Pessot, and G. A. Mourou, "Time-Resolved Observation of Electron-Phonon Relaxation in Copper," Phys. Rev. Lett. **58** (12), 1212 (1987).

[16] T. S. Eriksson, A. Hjortsberg, G. A. Niklasson, and C. G. Granqvist, "Infrared Optical-Properties of Evaporated Alumina Films," Appl. Opt. **20** (15), 2742 (1981).

[17] P. Yeh, *Optical Waves in Layered Media*. (Wiley, New York, 1988), p.406 p.

[18] T. N. Rhodin, "Low Temperature Oxidation of Copper. I. Physical Mechanism," J. Am. Chem. Soc. **72** (11), 5102 (1950).

[19] M. Sheik-Bahae, A. A. Said, T. H. Wei, D. J. Hagan, and E. W. Van Stryland, "Sensitive Measurement of Optical Nonlinearities Using a Single Beam," IEEE J. Quant. Elect. **26** (4), 760 (1990).

[20] M. Scalora, M. J. Bloemer, A. S. Pethel, J. P. Dowling, C. M. Bowden, and A. S. Manka, "Transparent, Metallo-Dielectric, One-Dimensional, Photonic Band-Gap Structures," J. Appl. Phys. **83** (5), 2377 (1998).

[21] K. Uchida, S. Kaneko, S. Omi, C. Hata, H. Tanji, Y. Asahara, A. J. Ikushima, T. Tokizaki, and A. Nakamura, "Optical Nonlinearities of a High Concentration of Small Metal Particles Dispersed in Glass: Copper and Silver Particles," J. Opt. Soc. Am. B **11** (7), 1236 (1994).

[22] M. Scalora, N. Mattiucci, G. D'auguanno, M. Larciprete, and M. J. Bloemer, "Nonlinear Pulse Propagation in One-Dimensional Metal-Dielectric Multilayer Stacks: Ultrawide Bandwidth Optical Limiting," Phys. Rev. E **73**, 016603 (2006).

[23] G. L. Eesley, "Generation of Nonequilibrium Electron and Lattice Temperatures in Copper by Picosecond Laser-Pulses," Phys. Rev. B **33** (4), 2144 (1986).

[24] P. E. Hopkins and P. M. Norris, "Substrate Influence in Electron-Phonon Coupling Measurements in Thin Au Films," Appl. Surf. Sci. **253** (15), 6289 (2007).

[25] A. N. Smith and P. M. Norris, "Influence of Intraband Transitions on the Electron Thermoreflectance Response of Metals," Appl. Phys. Lett. **78** (9), 1240 (2001).

[26] C. Voisin, N. Del Fatti, D. Christofilos, and F. Vallee, "Ultrafast Electron Dynamics and Optical Nonlinearities in Metal Nanoparticles," J. Phys. Chem. B **105** (12), 2264 (2001).